International Journal of Automotive Technology, Vol. 8, No. 3, pp. 361–373 (2007)

1229–9138/2007/034–13

STEADY-STATE OPTIMIZATION OF AN INTERNAL COMBUSTION ENGINE FOR HYBRID ELECTRIC VEHICLES

F. WANG*, T. ZHANG, L. YANG and B. ZHUO

Institute of Auto Electronic Technology, School of Mechanical Engineering, Shanghai Jiao Tong University, Shanghai 200240, China

(Received 17 November 2006; Revised 8 March 2007)

ABSTRACT–In previous work, an approach based on maximizing the efficiency of an internal combustion engine while ignoring the power conversion efficiency of other powertrain components, such as the electric motor and power battery or ultracapacitor, was implemented in the steady-state optimization of an internal combustion engine for hybrid electric vehicles. In this paper, a novel control algorithm was developed and successfully justified as the basis for maximal power conversion efficiency of overall powertrain components. Results indicated that fuel economy improvement by 3.9% compared with the conventional control algorithm under China urban transient-state driving-cycle conditions. In addition, using the view of the novel control algorithm, maximal power generation of the electric motor can be chosen.

KEY WORDS : Efficiency, Hybrid electric vehicles, Internal combustion engine, Steady-state optimization

NOMENCLATURE

n	: speed [r/min]
T	: torque [N.m]
P	: power [W]
be	: specific fuel consumption of ICE [g/kW.h]
$T_{ICE\_\max}'$	: torque of maximal efficiency of ICE@speed [N.m]
$T_{ICE\_\max}$	: maximal torque of ICE@speed [N.m]
T_{opt_pre}	: torque of SSO of ICE using the conventional algorithm [N.m]
P_{ge_pre}	: optimal generation power of EM using the conventional algorithm [W]
η	: efficiency during power transfer process path two
T_{opt}	: torque of SSO of ICE using the novel algorithm [N.m]
P_{ge}	: optimal generation power of EM using the novel algorithm [W]
V	: ultracapacitor voltage [V]

1. INTRODUCTION

There are six measures to improve fuel economy and reduce emissions in hybrid electric vehicles (HEVs). One such measure is that an internal combustion engine (ICE) runs at high efficiency points or regions (Oh *et al.*, 2005; Rousseau *et al.*, 2003; Park *et al.*, 2005). This can be achieved by steady-state optimization (SSO) of an ICE, which not only makes an ICE run more efficiently, but also maintains the charge of the power battery or ultracapacitor (Paganelli *et al.*, 2005). Because of the presence of an electric motor (EM), another power source, SSO of an ICE can be carried out by utilizing the genenominal characteristic of EM. The process of SSO of an ICE is: The ICE runs in one fixed original operating point, at which power production satisfies the power request of the drive and vehicle. Then the Electric Throttle Controller (ETC) of the ICE widens the throttle (Karnik, 2005). Thus ICE torque increases and the ICE speed remains constant. The increment of ICE torque or power can drive EM to charge the power battery or ultracapacitor, which will drive the vehicle at a suitable later time. In other words, SSO of an ICE is just like a driving generation control strategy. The difference is that the SSO of an ICE is the positive generation action to increase the ICE efficiency, regardless of the voltage of the power battery or ultracapacitor, as long as voltage is not beyond the upper limit; however, the driving generation is the passive generation action when voltage is below a logic threshold value.

Therefore, the HEV energy management (EM) control strategy in this study includes the SSO of ICE algorithm, but does not include a driving generation control strategy.

The questions that must be solved include: What is the optimal operating point of ICE? What is the optimal

**Corresponding author.* e-mail: wf51@sjtu.edu.cn

generation power of EM during the process of SSO of an ICE for an HEV?

The conventional classic control algorithm is based on maximizing the efficiency of an ICE. The conventional classic control algorithm did not provide much attention to efficiencies of other powertrain components, such as EM and power battery or the ultracapacitor in an HEV, and severe power conversion loss when it is transferred among overall powertrain components. Therefore, this previously developed control algorithm is not perfect and it is far from ready to be used in practical.

A major thrust of the paper is to discuss an approach and algorithm for the highest power conversion efficiencies and the least power conversion loss of the overall powertrain, rather than just maximizing the efficiency of an ICE when SSO of an ICE.

The remainder of this paper is organized as follows. Section 2 discusses the configuration of a specific HEV used throughout the paper and provides characteristics of the ICE and EM. Section 3 presents the conventional SSO of ICE control algorithm. Section 4 describes a novel control algorithm and compares the two algorithms using specific examples. Section 5 discusses some problems that should be solved for practical application. Section 6 presents primary results of this paper for fixed P_{GE_MAX} and different P_{GE_MAX} values. Finally, section 7 contains some conclusions and ideas for further work.

2. PARALLEL HYBRID ELECTRIC VEHICLE BASICS

The specific single shaft parallel integrated starter generator (ISG) hybrid electric vehicle configuration, which is used throughout the paper, is shown in Figure 1. Parameters of the vehicle and powertrain components are shown in Table 1.

The ICE and EM are two energy sources in a single shaft ISG HEV, the ICE is the main source. Therefore, two paths are used to drive the vehicle, shown in Figure 1 above. One is to use the ICE directly to drive the vehicle and the other is to use the EM to drive the vehicle. When the EM is used, energy comes from the ultracapacitor, which was charged earlier with the ICE (Niels *et al.*, 2003). Thus, when analyzing the use of the EM, the efficiency of the power flow from the ICE to the EM that is used as a generator, to the ultracapacitor during charging, and then from the ultracapacitor during discharging, to the EM that is used as a motor has to be analyzed.

Notations: $_{ICE}$ is used for the ICE; $_{EM}$ is used for the EM;

For our ISG HEV configuration, the maximal motor and generation efficiencies of the EM are 0.935, and the maximal charge and discharge efficiencies of the ultracapacitor are 0.985, so the least power loss is 0.935×0.935×0.985×0.985=0.85 for path two. Therefore, the power conversion loss is at least 15% for this specific ISG HEV.

Table 1. Parameters of the vehicle and powertrain.

Vehicle	Veh_mass	1300 kg
	Veh_CD	0.335
	Veh_FA	1.8m^2
	Wh_radius	0.19m
	Fd_ratio	4.308
	Gb_ratio	3.1820, 1.8590, 1.2500, 0.9090, 0.7030
ICE (Gasoline MR479QA)	Displacement	1.5L
	Max power	62kW@5900r/min
EM (Permanent magnet)	Maximal generation power (P_{GE_MAX})	6 kW
	Base speed	1500r/min
Ultracapacitor	Rated voltage	42V
	Capability	200F

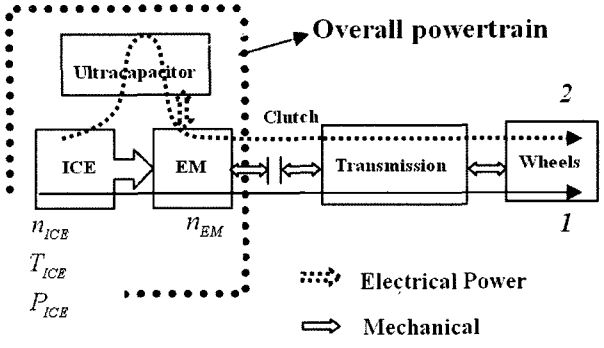

Figure 1. Configuration of a single shaft ISG parallel hybrid electric vehicle: using ICE directly (path one); using EM (path two).

It should be noted that the energy storage component in this study is an ultracapacitor, not a power battery. Because the charge and discharge efficiencies of the ultracapacitor are much higher than those of a power battery, the frequent and quick charge and discharge of an ultracapacitor are used. A quick charge means SSO of ICE, and a quick discharge means that the motor is assisted as much as possible.

Analysis from the bench test data provides characteristics of the 1.5L gasoline engine shown in Figure 2. It indicates that for a fixed n_{ICE}, the efficiency of the ICE increases with T_{ICE} increases until T_{ICE} reaches T_{ICE_max}'; unfortunately, it decreases when T_{ICE} is above T_{ICE_max}' to

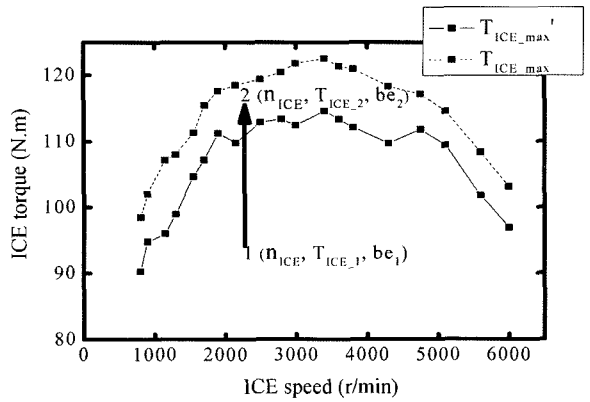

Figure 2. T_{ICE_max}' and T_{ICE_max} vs. n_{ICE}.

T_{ICE_max}.

For the EM, n_{EM} equals n_{ICE} and T_{EM} is the maximal generation torque under n_{EM} (Krause, 1987).

$$T_{EM}=\begin{cases}\dfrac{P_{GE\_MAX}\times 9550}{1500} & \text{If } n_{EM}\le 1500\ \text{r/min}\\ \dfrac{P_{GE\_MAX}\times 9550}{n_{EM}} & \text{If } n_{EM}>1500\text{r/min}\end{cases} \tag{1}$$

It is assumed that the ICE runs in operating point one and keeps n_{ICE} constant and then the ICE changes its operating point from one to two as shown in Figure 2.

Because of power restrictions of the ICE and EM, T_{ICE_2} under n_{ICE} is limited maximal up to T_x. Therefore, the constraint equations of the SSO of ICE control algorithm are:

$$T_x=\min[(T_{ICE\_1}+T_{EM}),T_{ICE\_\max}] \tag{2}$$

$$\forall T_{ICE\_2}\in[T_{ICE\_1},T_x] \tag{3}$$

3. CONVENTIONAL CONTROL ALGORITHM

The objective functions of the conventional SSO of ICE control algorithm are:

$$\mathbf{X}=be_2\ (T_{ICE\_2}) \tag{4}$$

$$Y=\min(\mathbf{X}) \tag{5}$$

Using the characteristics of the 1.5L gasoline engine and analyses from the above objective functions of the conventional algorithm and constraint equations, the detailed conventional classic SSO of ICE control algorithm includes:

(1) Algorithm one: When $T_{ICE\_1}+T_{EM}$ is greater than or equals to T_{ICE_max}', then the ICE can run in the operating point with the highest efficiency under n_{ICE}.Thus, SSO of the ICE operating point is:

$$T_{opt\_pre}=T_{ICE\_max}' \tag{6}$$

And P_{ge_pre} is smaller than or equal to P_{GE_MAX}, which is:

$$P_{ge\_pre}=\frac{(T_{ICE\_\max}'-T_{ICE\_1})\times n_{ICE}}{9.55} \tag{7}$$

(2) Algorithm two: When $T_{ICE\_1}+T_{EM}$ is smaller than T_{ICE_max}', then the ICE can not run in the operating point with the highest efficiency under n_{ICE}. Therefore, the SSO of ICE operating point and optimal generation power are:

$$T_{opt\_pre}=T_{ICE\_1}+T_{EM} \tag{8}$$
$$P_{ge\_pre}=P_{GE\_MAX}$$

4. NOVEL CONTROL ALGORITHM

4.1. Description

During power transfer process path two, the efficiency is computed as:

$$\eta=\eta_1\times\eta_2\times\eta_3\times\eta_4 \tag{9}$$

where η_1 is the generation efficiency of the EM; η_2 is the charge efficiency of the ultracapacitor; η_3 is the discharge efficiency of the ultracapacitor; and η_4 is the motor efficiency of the EM.

The increment of P_{ICE} between points one and two is P_{ICE_2}-P_{ICE_1}, but the useful P_{ICE} is $(P_{ICE\_2}$-$P_{ICE\_1})\times\eta$; power loss is $(P_{ICE\_2}$-$P_{ICE\_1})\times(1$-$\eta)$. Actually available P_{ICE} in the operating point two is $P_{ICE\_1}+(P_{ICE\_2}$-$P_{ICE\_1})\times\eta$, which can be used to drive the vehicle.

In addition, actual specific fuel consumption (be_2'), considering the power conversion efficiencies in operating point two of the ICE, is:

$$be_2'=\frac{be_2\times P_{ICE\_2}}{P_{ICE\_1}+(P_{ICE\_2}-P_{ICE\_1})\times\eta} \tag{10}$$

The simplification style for the constant n_{ICE} is:

$$be_2'=\frac{be_2\times T_{ICE\_2}}{T_{ICE\_1}+(T_{ICE\_2}-T_{ICE\_1})\times\eta} \tag{11}$$

Obviously be_2' is greater than be_2' for the power loss. Nevertheless, for operating point two, the relationship between be_2' and be_1 is unclear, and be_2' may be greater or smaller than be_1, or even equals to be_2'.

The ultimate goal of the novel SSO of ICE control algorithm is to determine how to find the optimal $T_{ICE\_2}(T_{opt})$ with minimal be_2' and optimal generation power of the EM (P_{ge}). Thus the actual peak efficiency of the ICE is found when power conversion efficiency is maximal and overall powertrain efficiency is the highest and power conversion loss is the least.

The objective functions of the novel SSO of ICE control algorithm are:

$$\mathbf{Be}=be_2'(T_{ICE\_2}) \tag{12}$$

$$B=\min(\mathbf{Be}) \tag{13}$$

Analyses from the above objective functions of the novel algorithm and constraint equations and the detailed novel control algorithm are as follows:

(1) Algorithm one: When B equals be_1, in other words:

$$[\forall be_2'(T_{ICE\_2})] \geq be_1 \tag{14}$$

then

$$T_{opt}=T_{ICE\_1} \tag{15}$$

$$P_{ge}=0 \tag{16}$$

No matter how much electricity is generated by the EM, the actual efficiency of the ICE decreases with the power conversion efficiency. Therefore, in this operating point, the SSO of ICE can not be carried out.

(2) Algorithm two: When B does not equal be_1, then there exists a minimal be_2' which makes the actual efficiency of the ICE maximal considering the power conversion efficiency. Therefore,

$$T_{opt}=T_{ICE\_2}(n_{ICE},\ T_{ICE\_1},\ B) \tag{17}$$

$$P_{ge}=\frac{(T_{opt}-T_{ICE\_1})\times n_{ICE}}{9.55} \tag{18}$$

4.2. T_{opt} and P_{ge}

Firstly, the ICE model was constructed using bench test data, calibrated by BOSCH®, of the 1.5L gasoline engine and Model-based Calibration Toolbox by MATHWORK® (Mathworks, 2005a). After assuring the validity of the ICE model, novel control algorithm based on this ICE model was formulated and implemented in the graphical environment of Simulink (Mathworks, 2005b). Figure 3 presents the simplified block diagram expression of the whole model of the novel control algorithm system.

Figure 3 shows that four input parameters are n_{ICE}, T_{ICE_1}, η and P_{GE_MAX}, and, for the expansibility of novel control algorithm, P_{GE_MAX} is selected as one input parameter. The first block interprets the speed and torque of the ICE as be and T_{ICE_max} using the ICE model, the second block is power restricted of powertrain; the third block computes the output T_{opt} and P_{ge} using the novel SSO control algorithm.

In addition, Figure 4 presents the flow chart of the

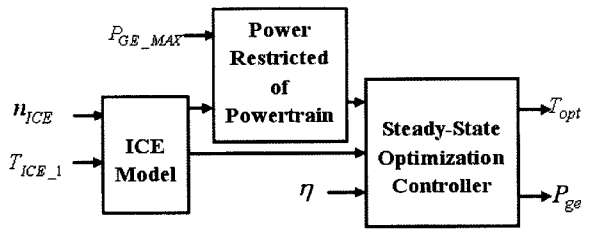

Figure 3. Simplified block diagram of the novel control algorithm.

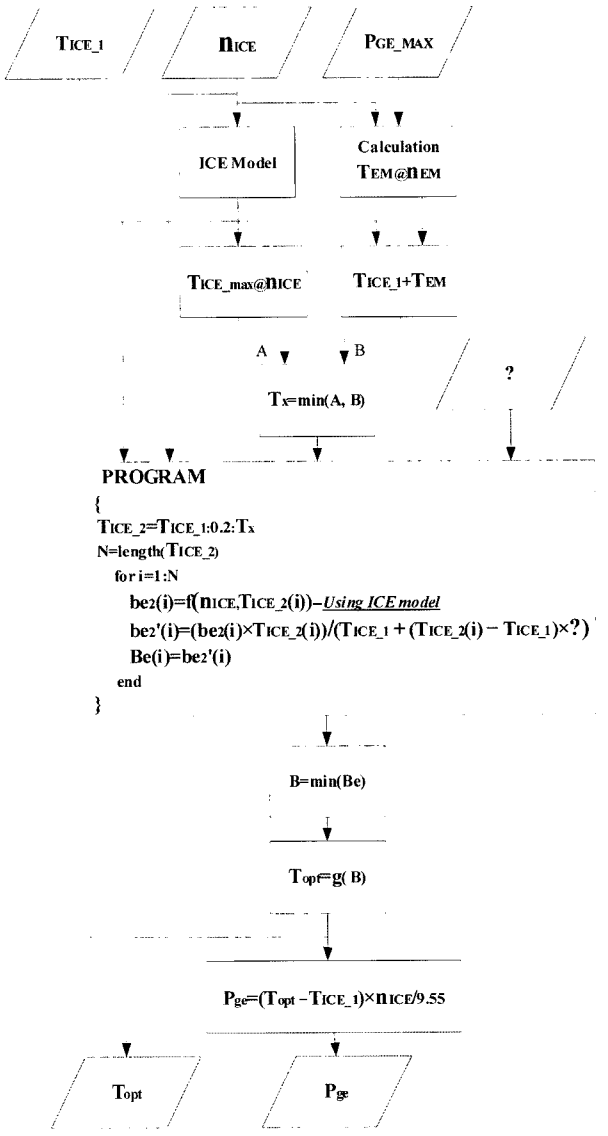

Figure 4. Flow chart of the novel control algorithm.

novel control algorithm. It gives the process of finding T_{opt} and P_{ge} for one original ICE operating point.

Using the model of the novel control algorithm above, T_{opt} and P_{ge} can be obtained for full scale operating points of the ICE. For convenience, the output T_{opt} and P_{ge} are stored in a two-dimensional array (MAP), which is based on T_{ICE_1} and n_{ICE}, according to different η, which is a series of discrete values from 0.5 to 0.8 with an equal interval.

Figure 5 and 6 illustrate the results of the novel control algorithm model with two MAPs. From Figure 6, it is seen clearly that for some operating points of the ICE, $P_{ge}$is zero. This case corresponds to the first novel control algorithm described above. For other operating points, P_{ge} is not zero and can be divided into two conditions.

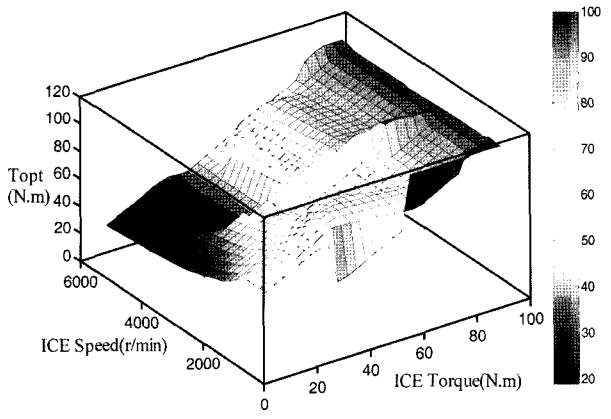

Figure 5. T_{opt} MAP when P_{GE_MAX}=6 kW, η=0.7.

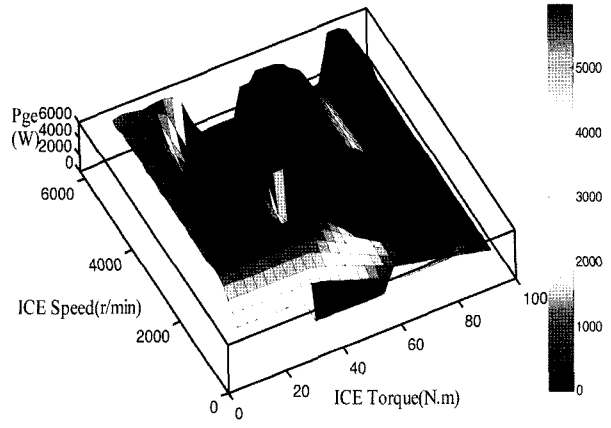

Figure 6. P_{ge} MAP when P_{GE_MAX}=6 kW, η=0.7.

One is that P_{ge} is P_{GE_MAX}; the other is that P_{ge} is smaller than P_{GE_MAX}. The two conditions correspond to the second novel control algorithm described above.

Some specific examples of the two above-mentioned cases are given as follows.

(1) Case One

In Figure 7, the example parameter is:

P_{GE_MAX} (kW)	n_{ICE} (r/min)	T_{ICE_1} (N.m)	η
6	3000	105	0.65

For

$$T_{ICE\_1}+T_{EM}=T_{ICE\_1}+\frac{P_{GE\_MAX}\times 9550}{n_{ICE}}=105+\frac{6\times 9550}{3000}$$

=124.1 N.m

T_{ICE_max}=121.8 N.m@3000r/min

Thus, the restricted torque scale of the powertrain is:

T_x=min[(T_{ICE_1}+T_{EM}), T_{ICE_max}]=min[124.1,121.8]=121.8N.m

The two dotted lines in Figure 7 represent the scale of restricted torque.

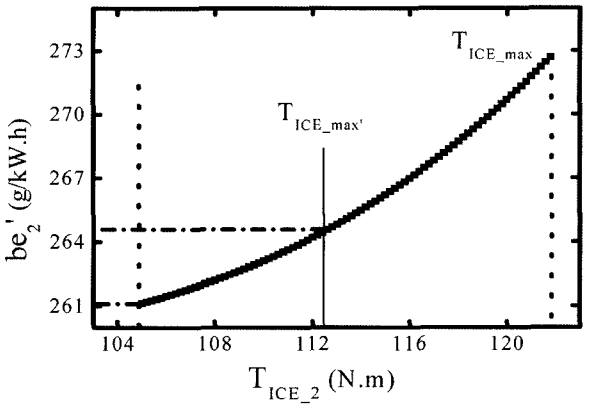

Figure 7. be_2' vs. T_{ICE_2}.

be_2' increases when T_{ICE_2} increases. Using the novel algorithm one:

T_{opt}=T_{ICE_1}=105N.m

P_{ge}=0 kW

Compared with the novel algorithm, the conventional algorithm yields

T_{ICE_1}+T_{EM}=124.1>112.5=T_{ICE_max}'

Thus, using conventional algorithm one,

T_{opt_pre}=T_{ICE_max}'=112.5 N.m@3000r/min

$$P_{ge\_pre}=\frac{(T_{ICE\_max}'-T_{ICE\_1})\times n_{ICE}}{9550}=\frac{(112.5-105)\times 3000}{9550}$$

=2.36 kW

(2) Case Two

a. Condition One

In Figure 8, the example parameter is:

P_{GE_MAX} (kW)	n_{ICE} (r/min)	T_{ICE_1} (N.m)	η
6	1600	35	0.7

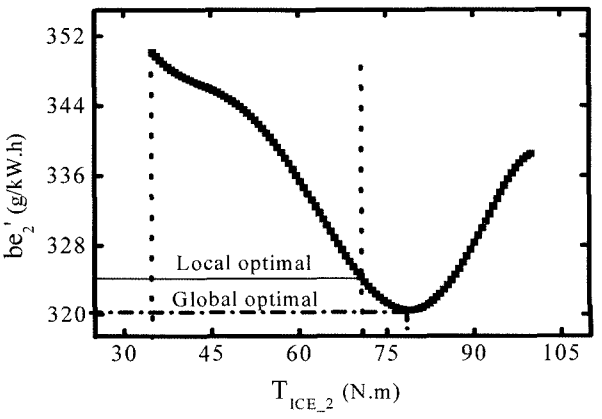

Figure 8. be_2' vs. T_{ICE_2}.

For

$$T_{ICE\_1}+T_{EM}=T_{ICE\_1}+\frac{P_{GE\_MAX}\times 9550}{n_{ICE}}=35+\frac{6\times 9550}{1600}=70.8 \text{ N.m}$$

T_{ICE_max}=112.7 N.m@1600r/min

Thus, the restricted torque scale of the powertrain is:

T_x=min[(T_{ICE_1}+T_{EM}), T_{ICE_max}]=min[70.8,112.7]=70.8 N.m

be_2' decreases continuously when T_{ICE_2} increases under the restricted power scale of the powertrain.
Then,

$T_{opt}=T_{ICE\_1}+T_{EM}$=70.8 N.m
$P_{ge}=P_{GE\_MAX}$=6 kW

Here the result of T_{opt} should be noted, because T_{opt} is just a local optimal result, not a global one. The global optimal result gains when P_{GE_MAX} is greater than 6 kW. There is a detailed explanation of this in section 6.2.

Compared with the novel algorithm, the conventional one yields

$T_{ICE\_1}+T_{EM}$=70.8<105.5=T_{ICE_max}'

Therefore, using conventional algorithm two,

$T_{opt\_pre}=T_{ICE\_1}+T_{EM}$=70.8 N.m
$P_{ge\_pre}=P_{GE\_MAX}$=6 kW

b. Condition Two
In Figure 9, the example parameter is:

P_{GE_MAX} (kW)	n_{ICE} (r/min)	T_{ICE_1} (N.m)	η
6	2000	60	0.75

For

$$T_{ICE\_1}+T_{EM}=T_{ICE\_1}+\frac{P_{GE\_MAX}\times 9550}{n_{ICE}}=60+\frac{6\times 9550}{2000}=88.65 \text{ N.m}$$

T_{ICE_max}=117.9 N.m@2000r/min
Thus, the restricted torque scale of the powertrain is:

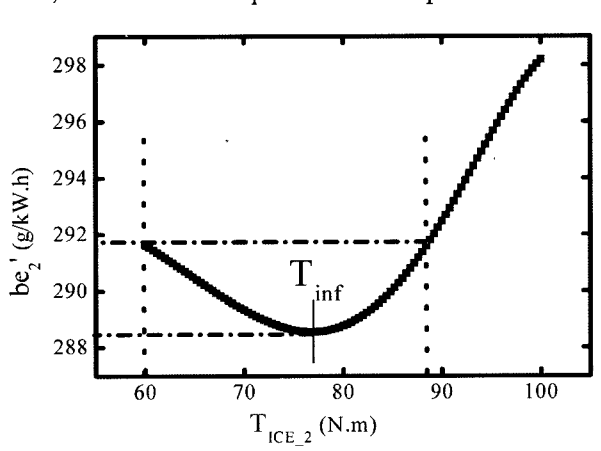

Figure 9. be_2' vs. T_{ICE_2}.

T_x=min[(T_{ICE_1}+T_{EM}), T_{ICE_max}]=min[88.68,117.9]=88.65 N.m

be_2' decreases firstly and then increases along with T_{ICE_2} under the restricted power scale of the powertrain, and there exists one inflexion, whose torque is T_{inf} and equals 76.8N.m. Therefore,

$T_{opt}=T_{inf}$=76.8N.m.

$$P_{ge}=\frac{(T_{inf}-T_{ICE\_1})\times n_{ICE}}{9550}=\frac{(76.8-60)\times 2000}{9550}=3.35 \text{ kW}$$

Here P_{ge} is smaller than P_{GE_MAX}.

Compared with the novel algorithm, the conventional one yields

$T_{ICE\_1}+T_{EM}$=88.65<110.66=T_{ICE_max}'

Thus, using conventional algorithm two,

$T_{opt\_pre}=T_{ICE\_1}+T_{EM}$=88.65N.m
$P_{ge\_pre}=P_{GE\_MAX}$=6 kW

4.3. Detailed Comparison
For the three examples shown above, a detailed comparison results of the two different control algorithms is reported in Table 2.

From the Table 2, for case one, the ICE can run at its maximal efficiency operating point under 3000 r/min. For the conventional algorithm, the ICE works in its maximal efficiency point, and the optimal generation power is 2.36 kW. η_{ICE} has been improved relative to non-SSO by 0.48%; however, η_{ICE} decreases more than non-SSO by 0.79%. Otherwise using the novel algorithm, the ICE in this operating point can not carry out SSO of an ICE, and the optimal generation power is zero. For condition one of case two, the ICE can not run at its maximal efficiency operating point under 1600 r/min. The effects are the same using conventional and novel algorithms and the optimal generation power is 6 kW; both η_{ICE} have been improved relative to non-SSO by 1.92%. For condition two, the ICE also can not run at its maximal efficiency operating point under 2000 r/min. Using the conventional algorithm, the optimal generation power is 6 kW. η_{ICE} has been improved relative to non-SSO by 2.54%; however, η_{ICE} decreases more than non-SSO by 0.01%. Using the novel algorithm, the optimal generation power is 3.35 kW. Though η_{ICE} has been improved relative to non-SSO by just 1.99%, which is less than when using the conventional algorithm; η_{ICE} has been improved relative to non-SSO by 0.31%.

It could concluded that although those η_{ICE} using the conventional control algorithm are always higher than or equal to those using the novel control algorithm, the results of η_{ICE} are contrary when considering power loss during power transfer through all of the powertrain components.

5. PROBLEMS BEFORE APPLICATION

Two major problems have to be addressed and those obstacles must be overcome before a fully practical application of SSO of ICE is achieved.

5.1. Calculation η

5.1.1. $\eta_3 \times \eta_4$

An additional research issue that remains to be tackled is value of $\eta_3 \times \eta_4$. In order to overcome the limitations due to the occurrence time of the EM assist and the unforeseen ultracapacitor discharge, the probability distribution and statistical analysis programs will be developed, which base their knowledge upon simulations in the lab or experimental data from chassis dynamometer tests of the specific driving-cycle.

In this study, based on the driving-cycle of China urban transient-state condition (detailed in Figure 14 below), using the simulation model for ISG_HEV (detailed in Figure13 below) for different values of initial voltage of the ultracapacitor, the efficiency of every working point of the EM motor and ultracapacitor discharge gained, then the average value of $\eta_3 \times \eta_4$ gained and was 0.85.

5.1.2. η_1 and η_2

η and η_2 are obtained through their own efficiency MAPs under the determined operating point of the EM generation and the ultracapacitor charge. η is based on the EM speed and generation power of the EM (Williamson, 2006); η_2 is based on power flowing into the ultracapacitor and work voltage of the ultracapacitor (V) (Jung *et al.*, 2003).

In this study, for prolonging the life-span and maintaining the high efficiency of the ultracapacitor, the constraint of V is:

$$30\text{V} \le V \le 50\text{V} \tag{19}$$

The EM speed and voltage of the ultracapacitor are achieved from the EM speed sensor and ultracapacitor control module. Power flowing into the ultracapacitor is P_{ge} multiplied η_1. However, P_{ge} is the output parameter of the SSO algorithm and is initially unknown. The relationship between them is just as in the following cycle.

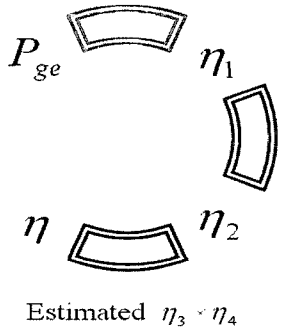

Table 2. Detailed comparison results.

	Case one			Case two				
				Condition one			Condition two	
	Non-SSO	SSO		Non-SSO	SSO		Non-SSO	SSO	
		Conventional algorithm	Novel algorithm		Conventional algorithm	Novel algorithm		Conventional algorithm	Novel algorithm
T_{opt} (N.m)		112.5	105		70.8	70.8		88.65	76.8
P_{ge} (kW)		2.36	0		6	6		6	3.35
be_1 (g/kW.h)	261.66			350.28			291.62		
be_2 (g/kW.h)		257.81	261.63		275.14	275.14		268.12	272.83
be_1' (g/kW.h)		268.22	261.63		324.37	324.37		291.67	288.55
$\Delta be=be_2'-be_1$ (g/kW.h)		6.56	0		-25.91	-25.91		0.05	-3.07
η_1	32.30%			24.13%			28.98%		
η_{ICE}		32.78%	32.30%		30.72%	30.72%		31.52%	30.97%
η_{ICE}'		31.51%	32.30%		26.05%	26.05%		28.97%	29.29%
$\Delta_{\eta_{ICE}}=\eta_{ICE}'-\eta_1$		-0.79%	0		1.92%	1.92%		-0.01%	0.31%

Notations: η_1, the non-SSO efficiency of the ICE; η_{ICE}, the SSO efficiency of the ICE without considering power loss; η_{ICE}, the actual SSO efficiency of the ICE considering power loss.

Table 3. Calculation process.

n_{ICE}=2000 r/min, T_{ICE_1}=60N.m, V=38 V, $\eta_3\times\eta_4$=0.85, N=6					
P_i (kW)	η_1	η_2	$\eta_1\times\eta_2$	η	P_i' (kW)
1	0.9050	0.9840	0.891	0.757	3.77
2	0.9031	0.9801	0.885	0.752	3.56
3	0.9033	0.9684	0.876	0.745	3.35
4	0.9040	0.9603	0.868	0.738	3.14
5	0.9038	0.9510	0.859	0.730	3.04
6	0.9009	0.9457	0.847	0.720	2.93

The practical solution is as follows. The assumed generation power of the EM can be from zero to P_{GE_MAX} (6 kW) divided into a series of discrete values P_i with equal intervals. Consider P_i for i=1,..., N, where N is the number of those discrete values.

Like the cycle above, each P_i concretely determines one η_1, and η_1 plus P_i determines the power flowing into the ultracapacitor, thus η_2 is obtained, then η is obtained using the estimated $\eta_3\times\eta_4$; finally the actual generation power of the EM (P_i') is obtained using SSO of ICE MAPs described above (Figure 6). As a result the other series of values P_i' are gained. Also consider P_i' for i=1,..., N.

Using the two series of discrete values, two curves with P_i and P_i' as functions of the index are obtained, and the point of intersection of the two curves is the optimal generation power P_{ge} in this status of overall powertrain components.

An example of the process to find the result of P_{ge} is reported in Table 3 and Figure 10.

Seen from Figure 10, P_{ge} is 3.3 kW. And

$$T_{opt}=T_{ICE\_1}+\frac{P_{ge}\times 9550}{n_{ICE}}=60+\frac{3.3\times 9550}{2000}=60+15.76$$

$$=75.76 \text{ N.m}$$

Moreover, Table 4 shows the efficiency improvement of

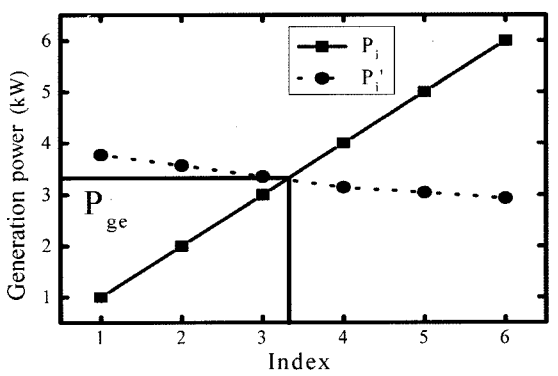

Figure 10. P_i and P_i' vs. Index.

Table 4. Efficiency improvement of the overall powertrain.

n_{ICE}=2000r/min, T_{ICE_1}=60N.m, V=38V, $\eta_3\times\eta_4$=0.85		
	Conventional algorithm	Novel algorithm
SSO of ICE point	(2000 r/min, 88.65N.m)	(2000 r/min, 75.76Nm)
η_{ICE}	31.52%	30.90%
η	72.00%	74.25%
Efficiency of overall powertrain	22.69%	22.95%
Improvement		0.26%

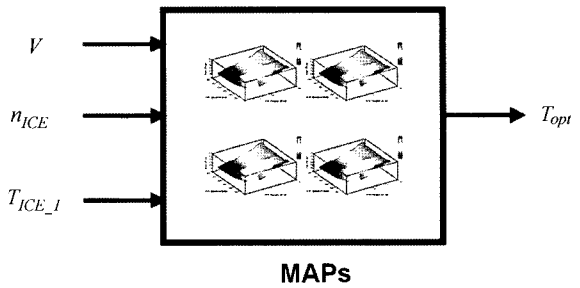

Figure 11. Input and output variables of novel SSO of ICE control algorithm.

the overall powertrain in the above- mentioned example. The overall powertrain efficiency improvement is 0.26% using the novel algorithm as compared with the conventional algorithm.

Using this method, for full scale operating points of the ICE, a series of MAPs for different values of V (30V to 50V) were obtained after off line calculation, shown in Figure 11, which stored in the Hybrid Control Unit (HCU) for practical application in order to satisfy the real time request of the control unit.

5.2. Inaccurate T_{ICE}

During SSO of an ICE, HCU should know T_{ICE} from the ICE Electric Control Unit (ECU) through CAN bus (Gerhardt *et al.*,1998). The problem is that T_{ICE} obtained from ECU is inaccurate, and the error is beyond the allowable tolerance, reaching ±10%. Figure 6 shows that inaccurate T_{ICE} will lead to two very different SSO of ICE.

For instance, in Figure 6, when n_{ICE} is 2800 r/min, the T_{ICE} value obtained from ECU is 50N.m whose optimal result is that P_{ge} equals 6 kW. Otherwise, the actual T_{ICE} value is 53N.m whose optimal result is that P_{ge} equals zero.

The results of those phenomena indicate that fuel

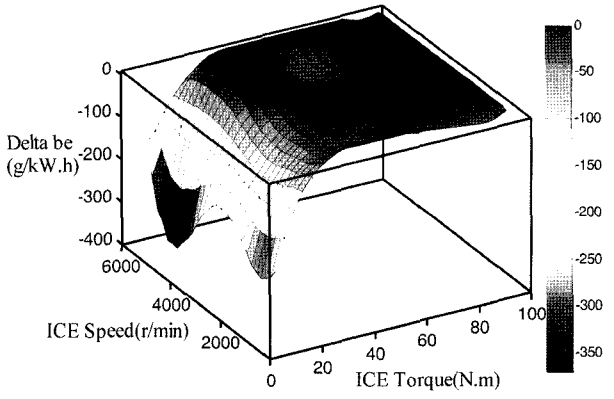

Figure 12. Δbe MAP when P_{GE_MAX}=6 kW, V=38V.

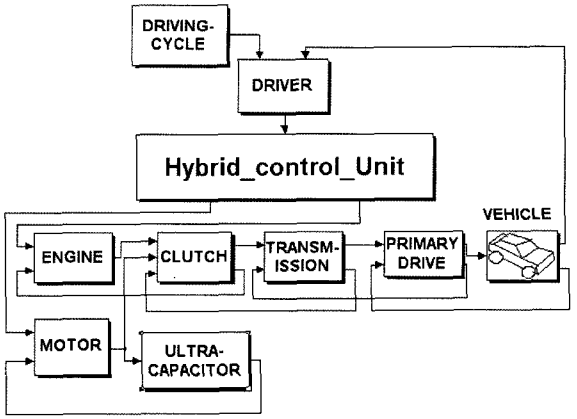

Figure 13. Top-level diagram of the ISG HEV simulation model.

consumption increases on the contrary compared with non-SSO of ICE. Therefore, the sensitivity analysis should be carried out in order to avoid this situation.

Set Δbe=min(be_2')-be_1, which means the quantity of saving *be* using the novel SSO of ICE control algorithm. Figure 12 shows one example of full scale operating points of the ICE.

For one operating point of ICE, it is assumed that the T_{ICE} obtained from ECU is *Tq_start*. Thus, the sensitivity analysis is as follows.

$$\forall T \in [(1-A)\times Tq\_start,\ (1+A)\times Tq\_start] \tag{20}$$

$$\forall V \in [30, 50] \tag{21}$$

$$\exists \left|\Delta be(n_{ICE}, V, T)\right| < M \tag{22}$$

where A and M are threshold values which can be calibrated, such as 0.1 and 5 g/kW.h.

If formula (22) above is satisfied, SSO of ICE in this operating point can not be carried out.

6. SIMULATION RESULTS

6.1. For Fixed P_{GE_MAX}

A forward HEV simulation model, which is implemented in SIMULINK, shows in Figure 13, developed at Shanghai Jiao Tong University is adopted to assess the performance of conventional and novel SSO of ICE algorithms.

In Figure 13, HCU mainly is energy management (EM) control strategy of HEV, which includes the SSO of ICE control algorithm mentioned in this study and other basic algorithms, such as the distribution of vehicle torque request between ICE and EM control algorithm, transient-state optimization of ICE control algorithm, EM assist control algorithm and regeneration braking control algorithm, ultracapacitor voltage-sustaining control algorithm, and so on.

For the fixed P_{GE_MAX}, 6 kW, simulations using the two different SSO of ICE algorithms, based on the above-

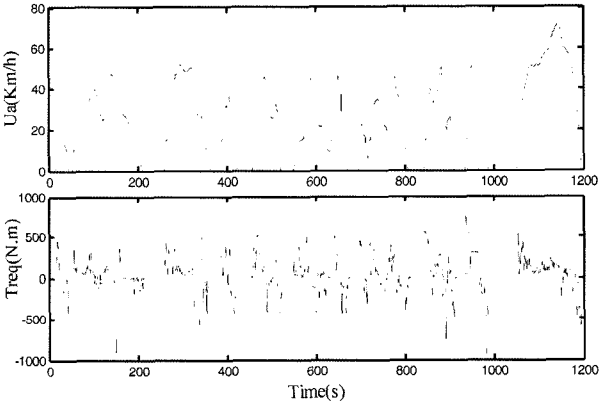

Figure 14. Driving-cycle of China urban transient-state conditions and vehicle torque request.

mentioned basic control algorithms, are developed. The initial V is 38V. The results are presented below using the driving-cycle of China urban transient-state conditions (CNDRC, 2006) shown in Figure 14. Curves of the vehicle velocity (U_a) and the vehicle torque request (T_{req}) are presented in Figure 14.

In addition, the limit conditions for occurrence and entrance of SSO of ICE are:

(At this moment, the EM state is idle) and ($V \leq 46$ V)

Otherwise, the limit conditions for exit of SSO of ICE are:

(At this moment, the EM state is motor or generation) OR ($V \geq 48$ V)

The simulation results presented in Figure 15 show that the ICE operating points (the ICE speed and torque) and corresponding happening time that can carry out SSO of ICE during the China driving-cycle. It also shows that the ICE operates mainly in low torque, low load rate and non-high efficiency range under current speed.

The solid and dotted curves in Figure 16 represent the

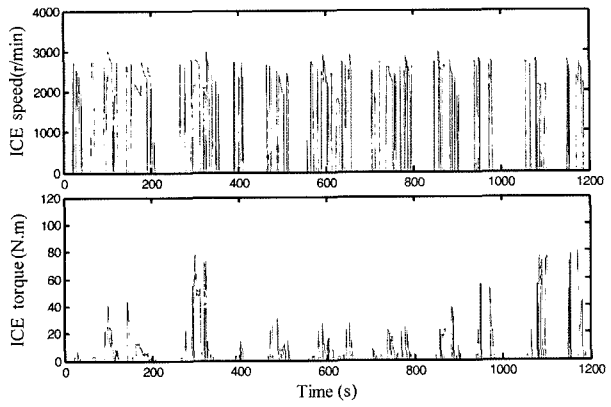

Figure 15. Speed and torque of the ICE operating points that can carry out SSO of ICE.

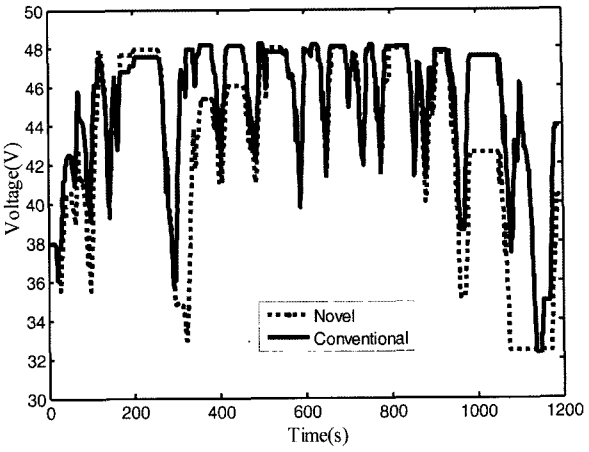

Figure 16. Ultracapacitor voltage.

voltage of ultracapacitor using conventional and novel algorithms respectively during the China driving-cycle with an initial V of 38V. It can be observed clearly that the SSO of ICE control algorithm is sufficiently able to maintain the work voltage of ultracapacitor. Many simulation results, using different initial V and driving-cycles, demonstrate the effectiveness of the SSO of ICE control algorithm in maintaining the work voltage of the ultracapacitor.

For the purpose of investigating further the behavior of the ICE, Figure 17 shows the SSO of ICE operating points for the two control algorithms. For the conventional algorithm, the SSO of ICE operating points are closer to the T_{ICE_max}'@n_{ICE} and the average efficiency of the ICE is higher than for the novel one.

Figure 18 and Figure 19 show the optimal EM generation powers and the EM operating points plotted on the EM efficiency map during the SSO of ICE. For the conventional algorithm, the generation powers are 6 kW mostly, only several points the generation powers are smaller, equal 3.0 kW; however for novel one, there are many points where generation powers are smaller than 6 kW and some of them are zero. Looking at efficiency maps of the EM, since the speed scale of the EM during SSO of ICE is only from 1500 r/min to 3000 r/min, in this speed area, the smaller generation power or torque leads to high generation efficiency of the EM.

Figure 20 presents the working points of the ultracapacitor plotted on the ultracapacitor efficiency map using the conventional and novel algorithms during SSO of ICE, respectively. They indicate that smaller charge power using the novel algorithm leads to the high efficiency charge process.

Therefore, the average of η_1 and η_2 is higher using the novel algorithm.

Table 5 presents the normalized losses and the fuel consumption of the vehicle for the China driving-cycle.

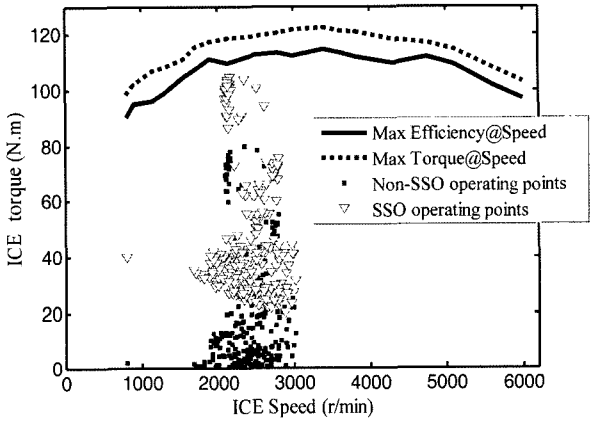

(a) Using the conventional algorithm

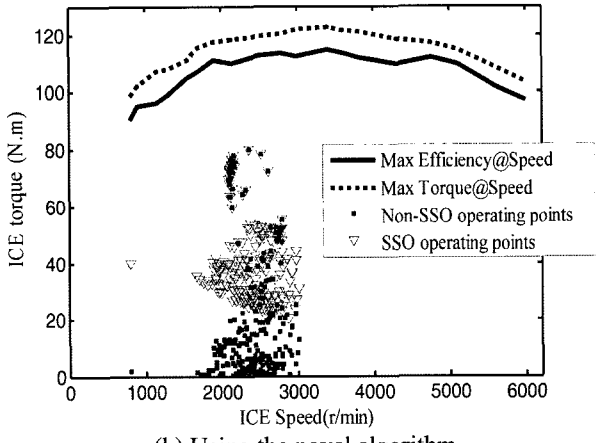

(b) Using the novel algorithm

Figure 17. Results of operating points of the ICE during SSO of ICE using (a) the conventional algorithm and (b) the novel algorithm.

The data in Table 5 demonstrate again that the novel algorithm is more effective than the conventional algorithm

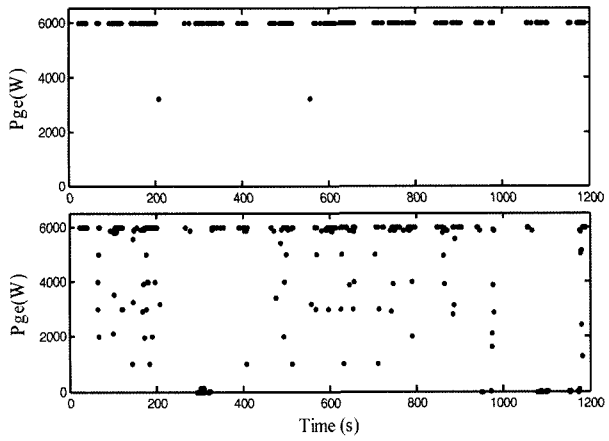

Figure 18. Optimization generation power of the EM during SSO of ICE. Above: using the conventional algorithm; Below: using the novel algorithm.

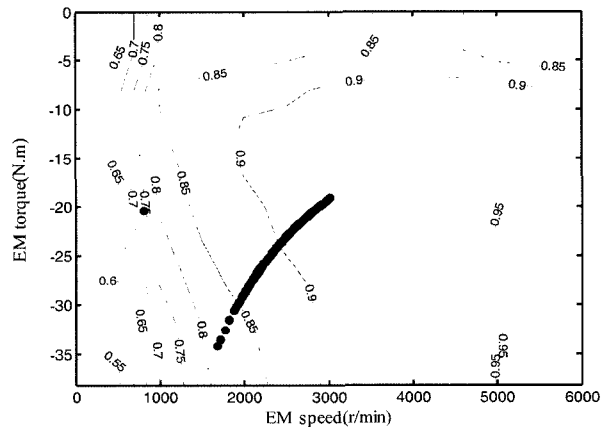

(a) Using the conventional algorithm

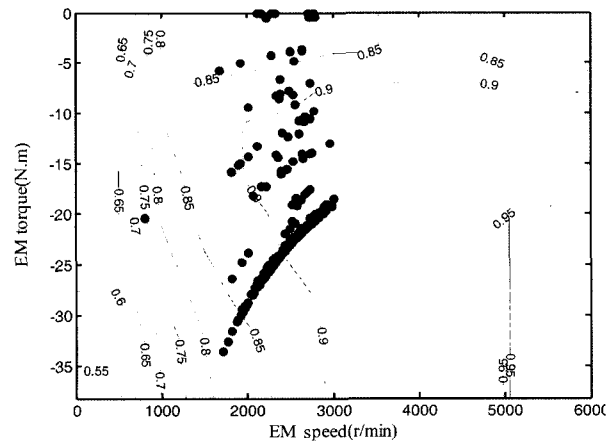

(b) Using the novel algorithm

Figure 19. Optimization of EM operating points during SSO of ICE using (a) the conventional algorithm and (b) the novel algorithm.

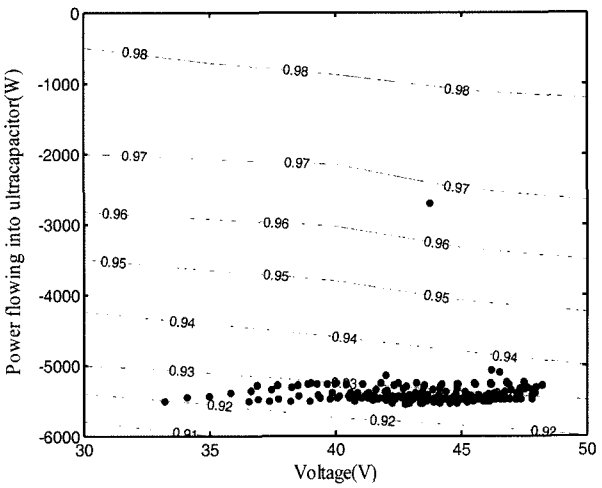

(a) Using the conventional algorithm

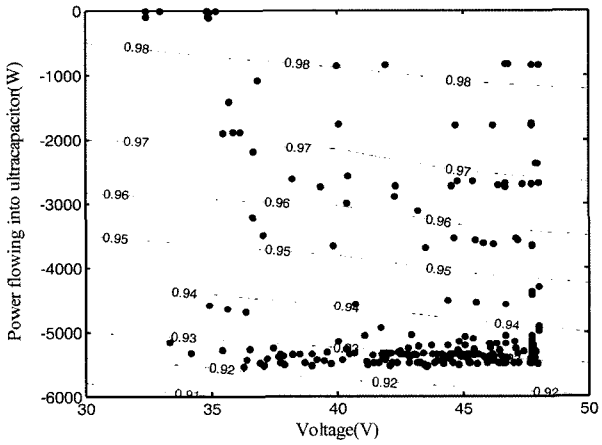

(b) Using the novel algorithm

Figure 20. Working points of the ultracapacitor during SSO of ICE using (a) the conventional algorithm and (b) the novel algorithm.

at maintaining the overall powertrain at higher efficiency. The losses are normalized with respect to the total loss for the conventional algorithm (which is 100%). The losses of drag, rolling resistance, energy for accessories, drivetrain and friction braking are approximately the same for the two control algorithms because they use the same vehicle and driving-cycle.

Table 5 shows that although the ICE average efficiency is a litter higher for the conventional algorithm, the ICE loss for the novel algorithm is smaller due to less fuel consumption. In addition, average efficiencies of others powertrain components of the novel algorithm are higher than those of the conventional one. Thus, there is a trade-off between the ICE efficiency and the efficiencies of the other powertrain components, and the power loss of the overall powertrain is smaller. Therefore, less fuel con-

Table 5. Normalized losses and the fuel consumption of the vehicle for conventional and novel SSO of ICE control algorithms.

Normalized losses	Novel algorithm	Conventional algorithm
ICE	62.8%	64.2%
EM	4.9%	6.8%
Ultracapacitor	2.6%	3.4%
Drivetrain	11.3%	11.3%
Rolling resistance	3.3%	3.3%
Drag	4.6%	4.6%
Accessories	2.1%	2.1%
Friction braking	4.3%	4.3%
Total	95.9%	100%
Initial V (V)	38.0	38.0
End V (V)	40.4	44.0
Fuel economy (mpg)	25.96	24.96
Fuel economy with V correction (mpg)	25.97	24.99
Fuel economy improvement		3.9%

sumption is needed to complete the cycle.

For the conventional and novel SSO of ICE control algorithms, fuel economy is 24.96 mpg and 25.96 mpg respectively. The voltage of the ultracapacitor jumps 6.0V for the conventional algorithm while this is only 2.4V for the novel one. Through six simulations over the same driving-cycle with different initial V from 32V to 42V, six sets of fuel economy and V change results are obtained. In order to calculate the corrected fuel economy corresponding to the zero V change over the China driving-cycle, a method of linear regression is used. The corrected fuel economy is 24.99 mpg and 25.97 mpg, respectively, for the conventional and novel SSO of ICE control algorithms. In addition, the impact on fuel economy is generally improved by 3.9%.

Fuel economy of the conventional vehicle, which has the same parameters as the specific ISG HEV, is 22.72 mpg. The impact on fuel economy is generally improved by 14.3% using the novel SSO of ICE and other basic algorithms of energy management.

The simulation research results are providing useful feedback information for improvements to the SSO of ICE.

6.2. For Different P_{GE_MAX}

For the determined 1.5L gasoline engine and its original operating point, if P_{GE_MAX} is infinite£¨there is a global optimal result of SSO of ICE, for which the actual specific fuel consumption is minimal. However, if P_{GE_MAX} is not great enough to run in that global optimal point, the result of SSO of ICE is not the global optimal, but rather it is the local optimal.

Figure 8 above shows that: when T_{ICE_2} is 78N.m, the global optimal result is obtained. However, P_{GE_MAX} is 6 kW and this restricted power prevents ICE from running at the global optimal operating point, therefore only a local optimal result is gained when T_{ICE_2} is 70.8N.m. If the global optimal result is sought, the expectation P_{GE_MAX} ($P_{GE\_MAX\_EX}$) should be greater than 6 kW and

$$P_{GE\_MAX\_EX} >= \frac{(78-35)\times 1600}{9550} = 7.2 \text{ kW}$$

When P_{GE_MAX} is infinite, for full scale operating points of the ICE, all of the results of SSO of ICE are global optimal; the actual specific fuel consumptions of the ICE are minimal and actual efficiencies of the ICE are maximal.

However, in actual applications P_{GE_MAX} is not infinite. A compromise in terms of the degree of SSO of ICE (i.e. the degree of fuel saving) and the cost of EM should be required.

Therefore, using the novel SSO of ICE control algorithm, P_{GE_MAX} can be chosen. Simulations were repeated with different P_{GE_MAX}, which varied from 3 kW to 30 kW and were infinitely added, as shown in Figure 21.

When P_{GE_MAX} is infinite, fuel economy improvement is 23.40% using the novel SSO of ICE and other basic algorithms of energy management, which is the greatest value for all different P_{GE_MAX}.

Figure 21 shows that as P_{GE_MAX} increases, the probability of a global optimal increases, and fuel consumption decreases. However, the slope of the curve becomes smaller and smaller, and the effect of fuel economy improvement becomes less and less distinctly.

Compared with the infinite generation power of the

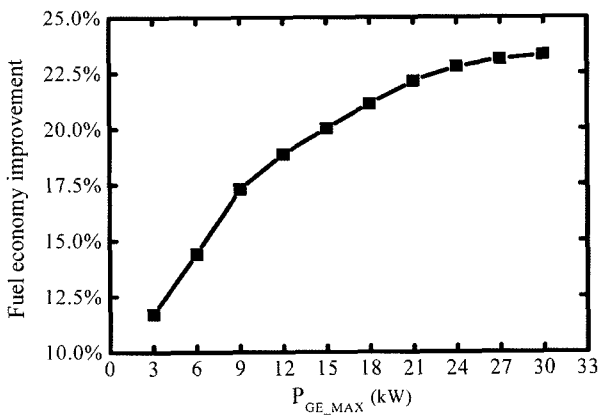

Figure 21. Fuel economy improvement vs. P_{GE_MAX}.

EM, a 6 kW EM has achieved a 61.1% impact on fuel economy improvement and 85.5% for a 15 kW EM.

7. CONCLUSION

The scope of this contribution was to introduce a novel control algorithm of SSO of ICE for HEV. Considering the power conversion efficiency of the overall powertrain, there is a trade-off between the ICE efficiency and the efficiencies of the other powertrain components. The ICE, EM and ultracapacitor efficiency MAPs of the powertrain components have been used to design the SSO of ICE control process.

Comparative simulations have been performed for the novel and conventional control algorithms using the driving-cycle of the China urban transient-state condition. They show that, using the novel algorithm, less power loss results in fuel economy improvement£¨and fuel economy improvement over the conventional default that only considers and optimizes the ICE efficiency by 3.9%. Moreover, P_{GE_MAX} can be chosen using the novel SSO of ICE control algorithm.

For the more effectual usage and practical application of SSO of ICE, further work should be done using the chassis dynamometer test for different driving-cycles to gain experimental data from which to obtain the value of $\eta_3 \times \eta_4$ since the data gained using the chassis dynamometer are more precise than that obtained by simulation.

The optimal idle operating point of ICE will be chosen using the same process of SSO of ICE for HEV in future research. It is our hope that considerably more work will be done in this area.

ACKNOWLEDGEMENT–This work was supported by the Electric Vehicle Key Project of Hi-Tech Research and Development Program of China (863) under contract No. 2002AA501700 and No. 2003AA501012. Also, the authors are grateful for the cooperation by New Energy Automobile Research Team in the Shanghai Maple Motor Company.

REFERENCES

CNDRC (2006). *Urban Driving-cycle in Automotive Experimentation*. Standard No: QC/T 759-2006. Chinese National Development and Reform Commission.

Gerhardt, J., Honninger, H. and Bischof, H. (1998). A new approach to functional and software structure for engine management systems-BOSCH ME7. *SAE Special Publications* **1357**, 197–208.

Jung, D. Y., Kim, A. W., Kim, S. W. and Lee, S. H. (2003). Development of ultracapacitor modules for 42-V automotive electrical systems. *J. Power Sources* **114**, **2**, 366–373.

Karnik, A. Y. (2005). Electronic throttle and wastegate control for turbocharged gasoline engines. *Proc. 2005 American Control Conf.*, **7**, 4434–4439.

Krause, P. C. (1987). *Analysis of Electric Machinery*. McGraw-Hill. New York.

Mathworks (2005a). *Model-based Calibration Toolbox 2.1.2 Edn*. The Mathworks Inc., Natick, Massachusetts, USA.

Mathworks (2005b). *Simulink. 6.2 Edn*. The Mathworks Inc., Natick, Massachusetts, USA.

Niels, J. S., Mutasim, A. S. and Naim, A. K. (2003). Energy management strategies for parallel hybrid vehicles using fuzzy logic. *Control Engineering Practice*, **11**, 171–177.

Oh, K., Kim, D., Kim, T., Kim, C. and Kim, H. (2005). Efficiency measurement and energy analysis for a HEV bench tester and development of performance simulator. *Int. J. Automotive Technology* **6**, **5**, 537–544.

Paganelli, G., Ercole, G., Brahma, A., Guezennec, Y. and Rizzoni, G. (2001). General supervisory control policy for the energy optimization of charge-sustaining hybrid electric vehicles. *JSAE Review* **22**, **4**, 511–518.

Park, C., Kook, K., Oh, K., Kim, D. and Kim, H. (2005). Operation algorithms for a fuel cell hybrid electric vehicle. *Int. J. Automotive Technology* **6**, **4**, 429–436.

Rousseau, A., Saglini, S., Jakov, M., Gray, D. and Hardy, K. (2003). Trade-offs between fuel economy and NOx emissions using fuzzy logic control with a hybrid CVT configuration. *Int. J. Automotive Technology* **4**, **1**, 47–55.

Williamson, S. S. (2006). Comprehensive drive train efficiency analysis of hybrid electric and fuel cell vehicles based on motor-controller efficiency modeling. *IEEE Trans. Power Electronics* **21**, **3**, 730–740.